AWARD NUMBER:
W81XWH-15-1-0719

TITLE: Automated Seat Cushion for Pressure Ulcer Prevention Using Real-Time Mapping, Offloading, and Redistribution of Interface Pressure

PRINCIPAL INVESTIGATOR: Muthu Wijesundara

CONTRACTING ORGANIZATION: University of Texas at Arlington
Arlington, TX 76019

REPORT DATE: October 2016

TYPE OF REPORT: Annual

PREPARED FOR: U.S. Army Medical Research and Materiel Command
Fort Detrick, Maryland 21702-5012

REPORT DOCUMENTATION PAGE

Form Approved
OMB No. 0704-0188

1. REPORT DATE	2. REPORT TYPE	3. DATES COVERED
October 2016	Annual	30 Sep 2015- 29 Sep 2016

4. TITLE AND SUBTITLE

Automated Seat Cushion for Pressure Ulcer Prevention Using Real-Time Mapping, Offloading, and Redistribution of Interface Pressure

5a. CONTRACT NUMBER

5b. GRANT NUMBER
W81XWH-15-1-0719

5c. PROGRAM ELEMENT NUMBER

6. AUTHOR(S)

Muthu Wijesundara, Rory Cooper

E-Mail:muthuw@uta.edu RCOOPER@pitt.edu

5d. PROJECT NUMBER

5e. TASK NUMBER

5f. WORK UNIT NUMBER

7. PERFORMING ORGANIZATION NAME(S) AND ADDRESS(ES)

The University Of Texas at Arlington
400 S Corn Street
Arlington TX 76019-0001

8. PERFORMING ORGANIZATION REPORT NUMBER

9. SPONSORING / MONITORING AGENCY NAME(S) AND ADDRESS(ES)

U.S. Army Medical Research and Materiel Command
Fort Detrick, Maryland 21702-5012

10. SPONSOR/MONITOR'S ACRONYM(S)

11. SPONSOR/MONITOR'S REPORT NUMBER(S)

12. DISTRIBUTION / AVAILABILITY STATEMENT

Approved for Public Release; Distribution Unlimited

13. SUPPLEMENTARY NOTES

14. ABSTRACT

The objective of the project is to realize an automated seat cushion that is capable of preventing the development of pressure ulcers by redistributing and offloading pressure based on real-time pressure mapping. In the first year, we focused on characterization of our soft bubble actuators capable of pressure redistribution as well as developed seat cushion testing prototypes. Fabrication techniques for the bubble actuators were developed and refined before integration into arrays for pressure redistribution testing. During the development the bubbles were characterized for their mechanical behavior at varying loads and internal pressures both by experimental testing as well as finite element simulation. Automation and control testing has been completed on a 5x5 array of bubble actuators to verify pressure redistribution performance. A complete seat cushion prototype has been completed and will be tested in the future work.

15. SUBJECT TERMS

Pressure ulcer prevention, automated seat cushion, bubble actuator, pressure modulation, pressure offloading, wheelchair cushion, spinal cord injury

16. SECURITY CLASSIFICATION OF:			17. LIMITATION OF ABSTRACT	18. NUMBER OF PAGES	19a. NAME OF RESPONSIBLE PERSON
a. REPORT	b. ABSTRACT	c. THIS PAGE			USAMRMC
Unclassified	Unclassified	Unclassified	Unclassified	34	19b. TELEPHONE NUMBER *(include area code)*

Contents

1 INTRODUCTION

The objective of the project is to realize an automated seat cushion that is capable of preventing the development of pressure ulcers by redistributing and offloading pressure based on real-time pressure mapping. In the first year, we focused on characterization of our soft bubble actuators capable of pressure redistribution as well as developed seat cushion testing prototypes. Fabrication techniques for the bubble actuators were developed and refined before integration into arrays for pressure redistribution testing. During the development the bubbles were characterized for their mechanical behavior at varying loads and internal pressures both by experimental testing as well as finite element simulation. Automation and control testing has been completed on a 5x5 array of bubble actuators to verify pressure redistribution performance. A complete seat cushion prototype has been completed and will be tested in the future work.

2 KEYWORDS

Pressure ulcer prevention, automated seat cushion, bubble actuator, pressure modulation, pressure offloading, wheelchair cushion, spinal cord injury

3 ACCOMPLISHMENTS

- **What were the major goals of the project?**

The overall goal of the project is to develop an automated seat cushion with real-time pressure mapping coupled with selective pressure offloading and dynamic redistribution to improve the standard of care for Spinal Cord Injury (SCI) individuals.

This goal will be accomplished by completing the following two aims:

Aim 1: Design and prototype a seat cushion using sensorized bubble actuators capable of real-time pressure mapping and modulation.

Aim 2: Conduct numerical and experimental studies on interface pressure and shear forces using an anthropomorphic model to develop a control algorithm.

First Year Milestones

1) **12 months milestone** (Cooper) Validate a sensorized anthropomorphic model using commercial wheelchair seat cushions (non-sensorized model completed, custom shear/pressure transducer completed, integration is pending. Some commercial seat cushion testing has been completed)
   60% complete
2) **24 months milestone** (Wijesundara) Build a sensorized seat cushion prototype and complete experimental testing (physical prototype completed, need to integrate control unit)
   60% complete
3) **30 months milestone** (Wijesundara) Develop a control unit capable of adjusting individual bubble actuator pressure to a preset value through the GUI (GUI for 5x5 array completed, testing in progress, extension to full seat cushion expected without issue)
   70% complete

4) **24 months milestone** (Wijesundara) Submit a paper describing an experimentally validated numerical model that predicts interface pressure and shear between an anthropomorphic model and a seat cushion prototype (initial data has been collected for two publications, draft preparation will occur in next reporting cycle)
   30% complete
5) **30 months milestone** (Wijesundara) Algorithms to identify anatomical features, recognize vulnerable areas based on pressure profiles and perform the pressure relief strategies (Initial pressure offloading and redistribution control algorithms have been developed for simplified test case)
   25% complete

- **What was accomplished under these goals?**

Accomplishments related to Aim 1: Design and prototype a seat cushion using sensorized bubble actuators capable of real-time pressure mapping and modulation.

Accomplishment #1: Design and fabrication of air filled bubble actuators and seat cushion prototype with strategic actuator placement for pressure modulation and redistribution

- **Specific objectives:**

1) Design actuators to achieve pressure offloading, modulation, and redistribution at different regions of the seat cushion.
2) Develop fabrication process for actuators that is both repeatable and scalable.
3) Design and fabricate a seat cushion layout for pressure offloading, modulation, and redistribution testing.
4) Study design optimization of the actuator based on two input parameters (the overall height and wall thickness of the actuators) and three output parameters (the maximum equivalent stress in the structure, vertical deformation in Y direction, and radial deformation in X direction).

- **Major activities:**

1) A cylindrical bubble actuator design was developed to offload and redistribute interface pressures by modulating inflation pressure in each bubble in the seat cushion array. The small circular profile of each actuator allows for a densely discretized array to measure and modulate interface pressures under the vulnerable areas of the user's body (i.e. under ischial tuberosity, coccyx, and sacrum).
2) Larger rectangular actuators were designed for placement under the thigh areas of the user, which are less vulnerable to pressure ulcer development. The function of these actuators is to shift overall load distribution across the entire seat cushion, rather than local offloading and redistribution. This allows for shifting of the weight of the user laterally or anteriorly/posteriorly, without fine control over pressure redistribution.

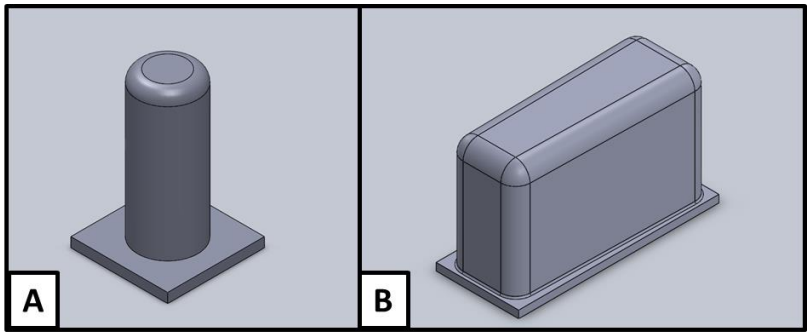

Figure 1 CAD models of bubble actuators A) Cylindrical bubble actuator for ischial region B) Rectangular actuator for thigh region

3) Developed a FE model in ANSYS for design optimization of the actuators. The overall height and wall thickness of the actuator were considered as the design parameters and the maximum equivalent stress

in the structure was selected for the optimization of objective function. The procedure includes four steps, I) Mechanical Model Development: set up a mechanical model of the actuators and a plate that simulates the interaction between an external object with a single actuator (See Figure 2). The simulation for the Design Optimization test setup includes half of a single bubble actuator, half a plate at the top, zero displacement for the symmetry boundary condition and the side walls of the plate, a fixed support at the base, and application of uniform pressure on the whole plate and HSFLD elements to replicate the air contained in the bubble, as shown in Figure 2. In addition, a frictional contact condition has been considered for the interaction between the bubble actuator and the bottom side of the plate (friction coefficient: 0.8). A static FE analysis was carried out in two loading steps: 1) the pressure of the HSFLD was set to the specified initial pressures (7.0 kPa), and 2) a uniform pressure (3.5 kPa) was applied to the top surface of the plate to produce approximately 20.0 kPa interface pressure between the plate and the actuator based on the peak sitting interface pressures. The results including the maximum equivalent stress, the deformation in X direction (radial), and the deformation in Y direction (vertical) were recorded, II) Design of Experiment: 10 design points (Height, Wall Thickness) were selected (see Table. 1) where the height and the wall thickness vary between 50mm to 75mm and 0.75 mm to 1.25mm, respectively, then a FE static structural analysis was carried out for each design point to calculate the equivalent stress for further analysis. III) Surface Response: A predictive model was fitted to the results of the design points in order to realize a continuous response function for the variation range of input parameters, and finally, IV) Optimization: Genetic algorithm based optimization was performed on the collected data in order to find the optimal design which minimizes the maximum equivalent stress in the actuators.

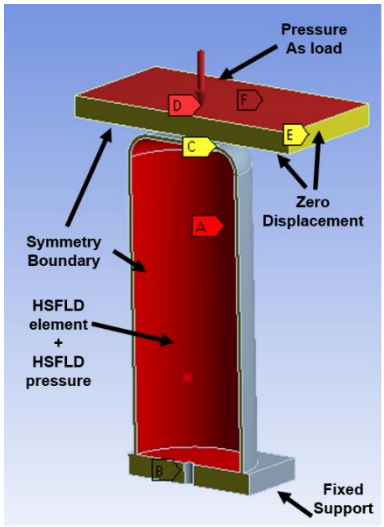

Figure 2 The Simulation setup that demonstrates the boundary conditions and loading for the design optimization.

Table 1 The selected design points

Wall Thickness (mm)	Height (mm)
0.75	62.5
0.75	50
0.75	75
1	62.5
1	50
1	75
1.25	62.5
1.25	50
1.25	75

4) Developed polyurethane rubber molding processes for both cylindrical and rectangular actuator elements. Two molding processes have been developed to produce the actuators: 1) Injection molding: This process allows for rapid prototyping for iterative design changes, and 2) Rotational molding: This process can be completed in a single step to accelerate actuator production. The development included 3D CAD modeling to design the mold assemblies and process refinement to ensure consistent production. The molds were 3D printed using the CAD designs to define the desired actuator dimensions. Process development included how to pre-process the polymer before injection, multi-step molding processing, rotational speed and duration, as well as curing time and temperature.

5) Designed the initial seat cushion conceptual design with differing actuator shapes and placement for both overall load shifting and fine pressure redistribution. The seat cushion design shown in Figure 3 utilizes a dense array of cylindrical actuators in the ischial region to allow for pressure redistribution with a highly discretized resolution. This is critical in the vulnerable ischial region where the bony prominences of the sit bones highly compress the soft tissue, leading to pressure ulcer development. Conversely, the rectangular actuators under the thigh regions can be inflated or deflated individually to shift the user's weight laterally or in tandem to shift load distribution anteriorly/posteriorly. The actuators are constrained from collapsing outward by the foam supports around the perimeter of the seat cushion. Furthermore, the contouring of the foam is intended to help center the user on the actuator array and accommodate variations in thigh and buttocks width between users.

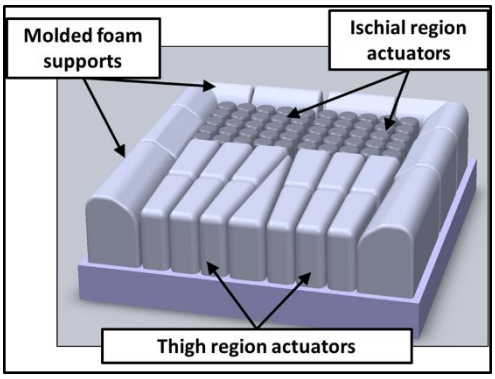

Figure 3 Conceptual model of seat cushion layout designed for optimal pressure redistribution

6) To facilitate electronic pressure controller development and preliminary pressure redistribution testing, a 5x5 quarter seat cushion actuator array was fabricated and assembled. The advantage of constructing the test platform is to allow parallel development of electronic controller and control algorithms while entire seat cushion design was finalized.

- **Significant results:**

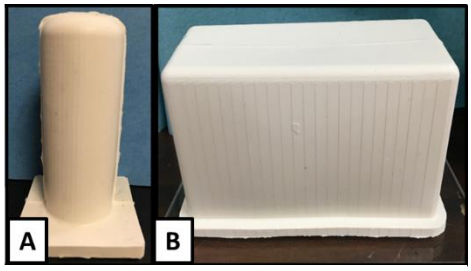

Figure 4 Fabricated polyurethane rubber bubble actuators A) Cylindrical actuator B) Rectangular actuator

Designed pressure modulating bubble actuators

The preliminary actuator designs, pictured in Figure 4 and prior to design optimization, include the cylindrical actuator for placement under the ischial region and the rectangular actuator for placement under the thigh region. These actuators can tolerate internal air pressures up to approximately 28 kPa without failing. The dimensions of the cylindrical actuator are 30mm in diameter and a height of 75mm. The dimensions of the rectangular actuator are 129x50x75mm.

Obtained finalized design parameters for cylindrical actuators

1) In the Table 2 FE analysis results, the Output Parameter ranges for equivalent stress, radial deformation, and vertical deformation are presented alongside their Input Parameters, overall height and the wall thickness. Figure 5(a) and (b) show the deformation and stress distribution of a single actuator under loading, respectively.

Table 2. The FE analysis results

Input Parameters		**Output Parameters**		
Wall Thickness (mm)	**Height (mm)**	**Equivalent Stress (MPa)**	**Radial deformation (mm)**	**Vertical deformation (mm)**
0.75-1.25	50-75	0.273 to 0.406	1.8-3.03	6.3-11.8

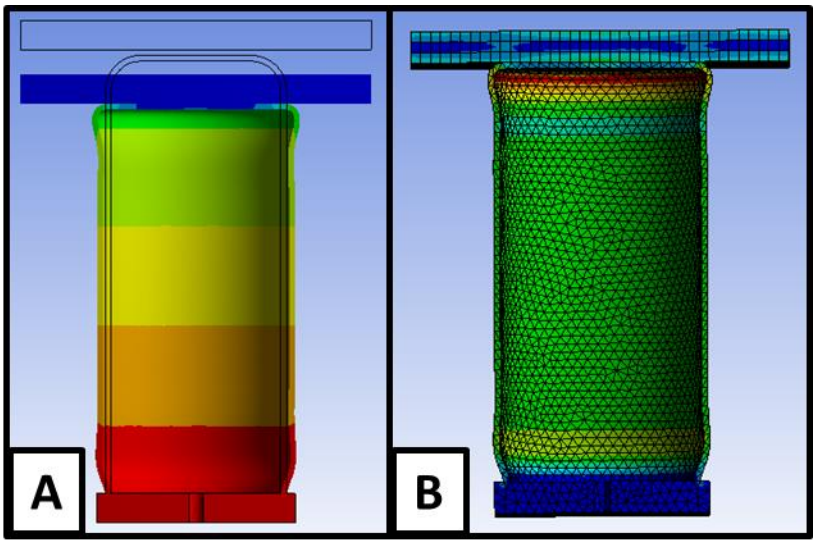

Figure 5 (A) Deformation of the actuator in Y direction under an external pressure loading for the design point (WT = 1.0 mm and H = 61.5mm), (B) Equivalent stress distribution in the actuator under an external pressure loading for the design point (WT = 1.0 mm and H = 61.5mm)

2) Figure 6 shows the surface response of the output parameters with respect to the variation of the input parameters. These surfaces were fitted to the results obtained by the individual design points. Figure 6(A) and (B) show that the equivalent stress and the radial deformation have similar trend where their optimal value (which in this case is the minimum) occurs when the height is at the lower and the wall thickness is at the upper bound of the range. However, for the vertical deformation, the optimum (which in this case is the maximum) deformation happens when the height is at the upper and the wall thickness is at the lower bound of the range. Therefore, it is impossible to have a three-way optimization for these output parameters and instead an individual optimization study was carried out for each output parameter.

3) The results for the design optimization of the actuators for each output parameters are shown in Table 3. A genetic algorithm based optimization technique was implemented to find the optimum values of the output parameters and corresponding design parameters using the surface responses (Figure 6).

Table 3. The design optimization results:

	Equivalent Stress(0.27 MPa)	**Radial Deformation (1.81mm)**	**Vertical Deformation (11.65mm)**
Height (mm)	60.7	51.9	74.4
Wall Thickness (mm)	1.23	1.24	0.76

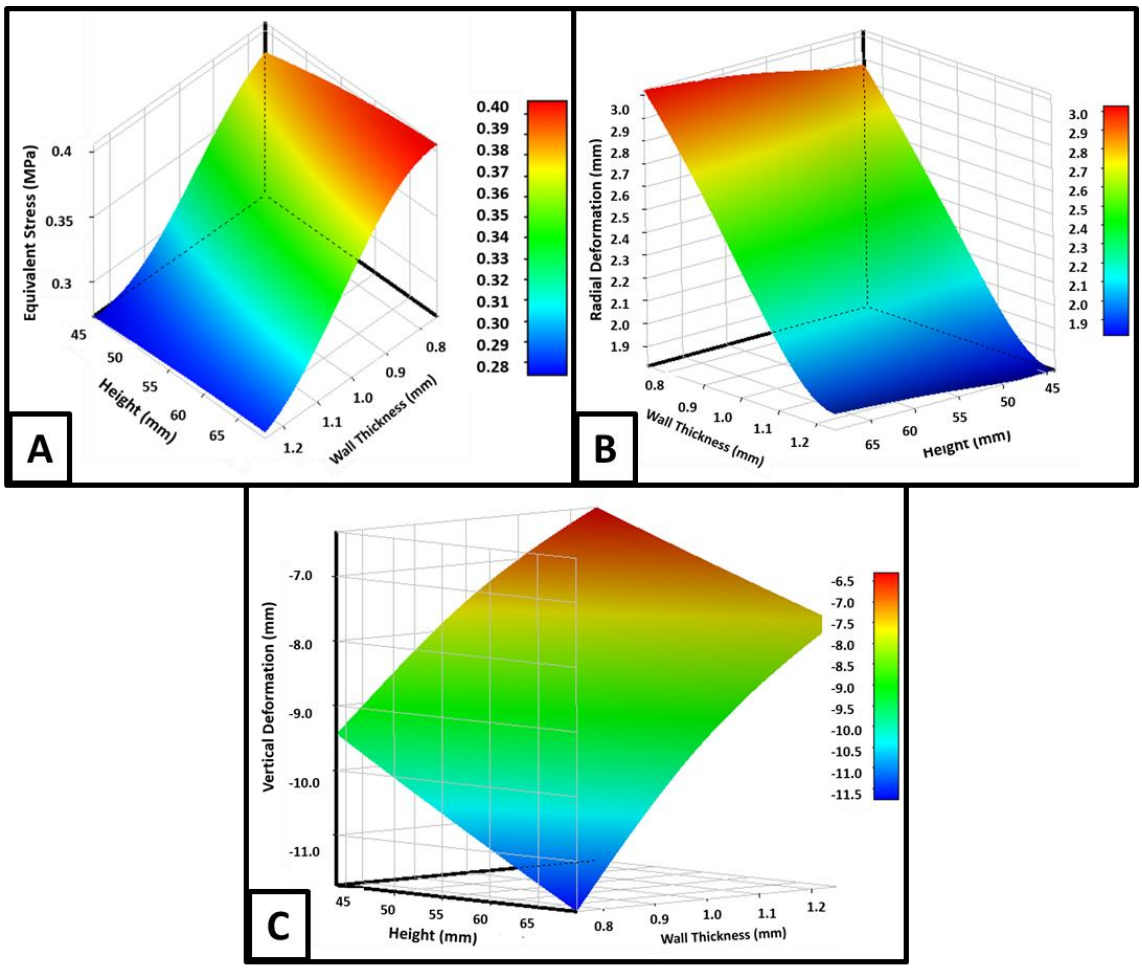

Figure 6 (A) Surface response of the maximum equivalent stress in the actuator structure with respect to the inputs parameters variation, (B) Surface response of the radial deformation of the actuator (X direction), and (C) Surface response of the vertical deformation of the actuator (Y direction).

Actuator fabrication using liquid polyurethane rubber molding process

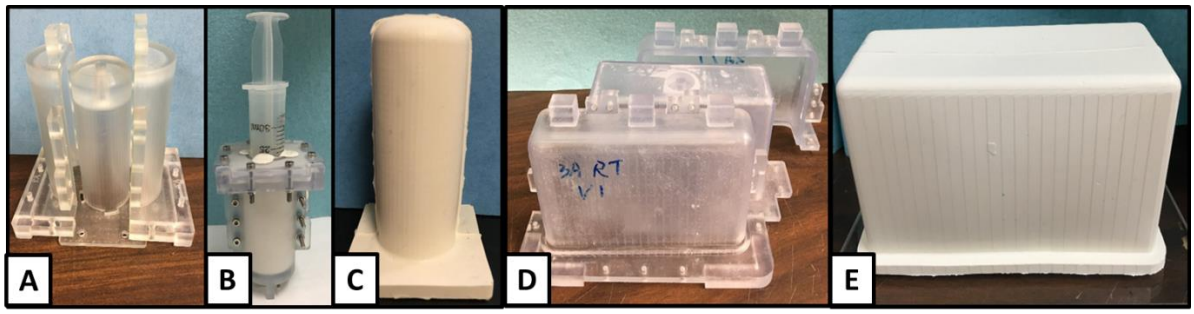

Figure 7 Injection molding process of actuators A) Three-part cylindrical actuator mold B) Cylindrical actuator being molded by injection via syringe C) Molded cylindrical actuator D) Three-part rectangular actuator mold E) Molded rectangular actuator

1) Injection molding process:

Both actuators have been fabricated using an injection molding process of the liquid polyurethane rubber and 3D printed molds. The molds are assembled as three parts with two exterior pieces to define the outer surface of the actuators and a solid core to maintain the cavity of the actuator. After molding the actuator, the core is removed and a base is molded with a molded airline for inflation and deflation. The process is straightforward, produces actuators of consistent wall thickness, and has a low defect rate. The use of 3D printed molds allows for quick turnaround with iterative design changes and cheap replication to increase production.

2) Rotational molding process:

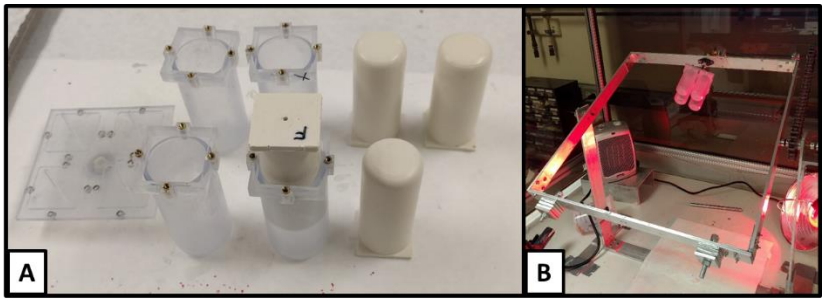

Figure 8 Rotational molding process A) Two-part mold for 4 cylindrical actuators B) Two-axis rotational molding of cylindrical actuators in heated chamber

The rotational molding process has been finalized which eliminates the need for the two step process described above and allows for simultaneous production of four actuators. The process involves introducing the liquid polyurethane rubber into the cavities shown in Figure 8A and rotating them in a heated chamber (Fig 8B) until an even coating has been achieved on the interior surface of the mold. Since there is no need for a three part mold with a solid core, the exterior parting line seen in Fig 7C can be eliminated to produce a smooth outer bubble surface. The mold has cavities for four actuators and rotates on a custom built two-axis rotational coating system to ensure even coating across all surfaces. The actuators can then be simply removed from the mold, with the base and airline already molded in place, without the need to remove them from a solid core and subsequently mold the base. This process greatly improves the efficiency of production by simplifying to a one-step high throughput process.

Designed and fabricated seat cushion prototype platform

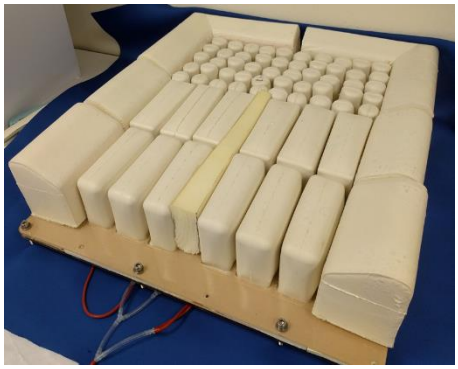

Figure 9 Assembled seat cushion prototype

The completed seat cushion prototype is shown in Figure 9. It is constructed on an acrylic sheeting base which maintains actuator alignment and routes the pneumatic lines downward for interfacing with the electronic pressure controller. The overall dimensions of the seat cushion are 480mm(W) x 480mm(D) x 97.5mm(H). All of the actuators are made from polyurethane rubber as described above and the foam pieces are molded from a polyurethane foam and coated with polyurethane rubber to prevent tearing.

Figure 10 5x5 quarter seat cushion actuator array for testing

Designed and fabricated quarter seat cushion 5x5 actuator array for initial pressure offloading algorithm development and testing

A completed 5x5 quarter seat cushion actuator array has been completed and is shown in Figure 10. The array takes advantage of the symmetry of the seat cushion design to allow us to perform pressure redistribution testing for half of the ischial region. Similar to the entire seat cushion, the actuators are assembled upon an acrylic base which also routes the pneumatic lines underneath the platform.

Accomplishment #2: Simulation and experimental characterization of actuator mechanical behavior.

- **Specific objectives:**

1) Validate a developed ANSYS simulation model to predict actuator mechanical behavior by comparing with experimental high accuracy pointwise deformation measurements
2) Use the validated ANSYS simulation model to obtain the mechanical characteristics of the actuators at different actuation pressures for control scheme development.

- **Major activities**:

1) A finite element (FE) model of the bubble actuator was developed in the commercial software ANSYS in order to determine the deformation of the actuator in a free expansion condition. The simulation setup, as shown in Fig. 11(a) for the deformation-based model validation includes a half of a single bubble actuator, zero displacement for the symmetry boundary condition, fixed support at the base, and hydrostatic fluid (HSFLD) elements used to replicate the air contained in the actuator. The pressure of the HSFLD is varied from 0-25kPa with 2.5kPa increments in a steady-state finite element analysis and the displacement of 6 markers shown in Fig. 11(b) are recorded.
2) To validate the simulation results (pressure vs pointwise deformation data) obtained by the FE model, a high accuracy optical recognition setup as shown in Fig. 12(a) was used to carry out the deformation test based on pointwise deformation measurements. Black hemispherical markers with a diameter of 4mm were used in corresponding to the points TR, TC, MR, MC, BR, BC shown in Fig. 12(b). The perpendicular placement of cameras allows for observation of x, y, z coordinates of all six points of interest, shown in Fig. 12(c).
3) Raw images from the two perpendicularly mounted cameras are captured as shown in Fig. 12(b) and then analyzed through a series of MATLAB image processing routines to identify, sort, and track the location of the intended points (markers), Fig. 12(c). Further, magnification factor is calculated after accounting for spherical aberrations and perspective transformation. As a result displacements in the Cartesian space can be measured with subpixel accuracy. This procedure is repeated for internal gauge pressures from 0-25kPa with 2.5kPa increments. Note that the deformation at any particular pressure is calculated by subtracting the position with its counterpart at zero gauge pressure. Data are collected for three different samples of the actuator to capture an average behavior. The whole experiment is repeated three times to ensure repeatability.

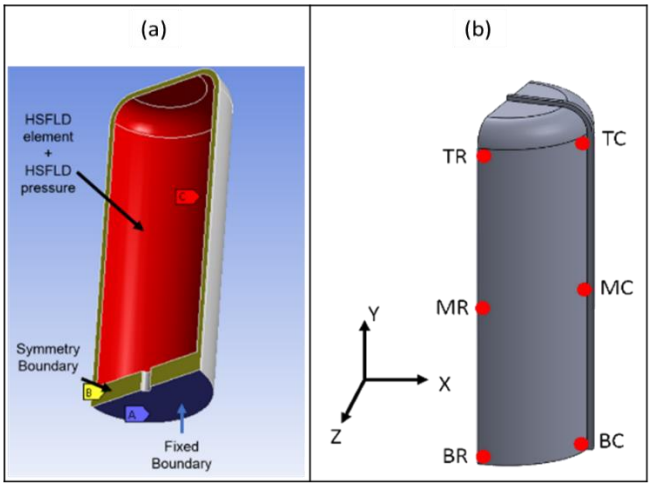

Figure 11 (a) Schematic of conditions used for the ANSYS model to simulate free expansion; (b) Locations of markers on the actuator at TR, TC, MR, MC, BR.

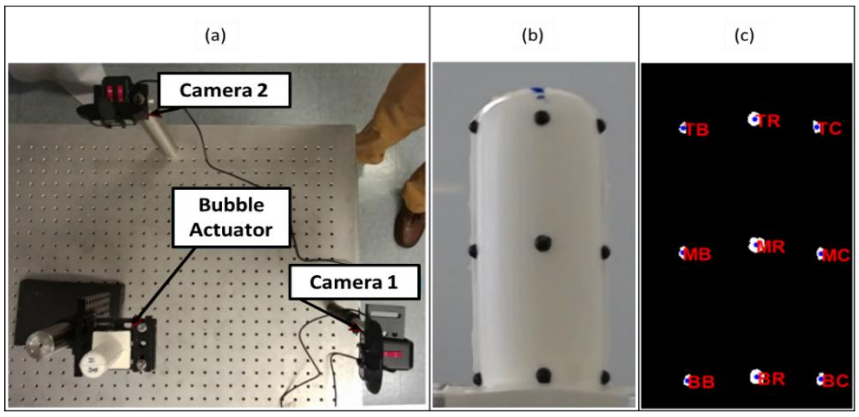

Figure 12 (a) Bench-test setup to capture pointwise actuator deformation, (b) Raw cropped image from Camera 2 at 2.5kPa, and (c) Processed image from Camera 2 at 2.5kPa.

4) To determine the mechanical characteristics of the actuators at different actuation pressures, six samples of bubble actuators were tested repeatedly, using the force-pressure setup (see Figure 13(a)) and the mechanical behavior is documented. The continuous time measurements of internal gauge pressure, interface force, and displacement were recorded for an actuator responding to a commanded deformation in the Y direction with the pneumatic system being closed. For each actuator sample, such behavior was recorded at initial internal pressures varying from 2.5-25kPa with 2.5kPa increment. The whole procedure was repeated three times to ensure repeatability.
5) A FE model was developed in ANSYS to replicate the experimental setup. Force interaction model was used to corroborate the force, pressure, and deformation measurements. The simulation for the force test setup includes a half of a single bubble actuator, a half plate at the top, zero displacement for the symmetry boundary condition and the side walls of the plate, fixed support at the base, displacement of the whole plate and HSFLD elements to replicate the air contained in the bubble, as shown in Fig. 13(b). In addition, a frictional contact condition has been considered for the interaction between the bubble actuator and the bottom side of the plate (friction coefficient: 0.8). A static finite element analysis was carried out in two loading steps: 1) the pressure of the HSFLD elements was set to the specified initial pressures (2.5, 5.0, 7.5…25kPa), and 2) the plate will be displaced for a specific distance based on the experimental setup (Fig. 13(a)). The results including the internal pressure change and the forces at the contact surface were recorded.

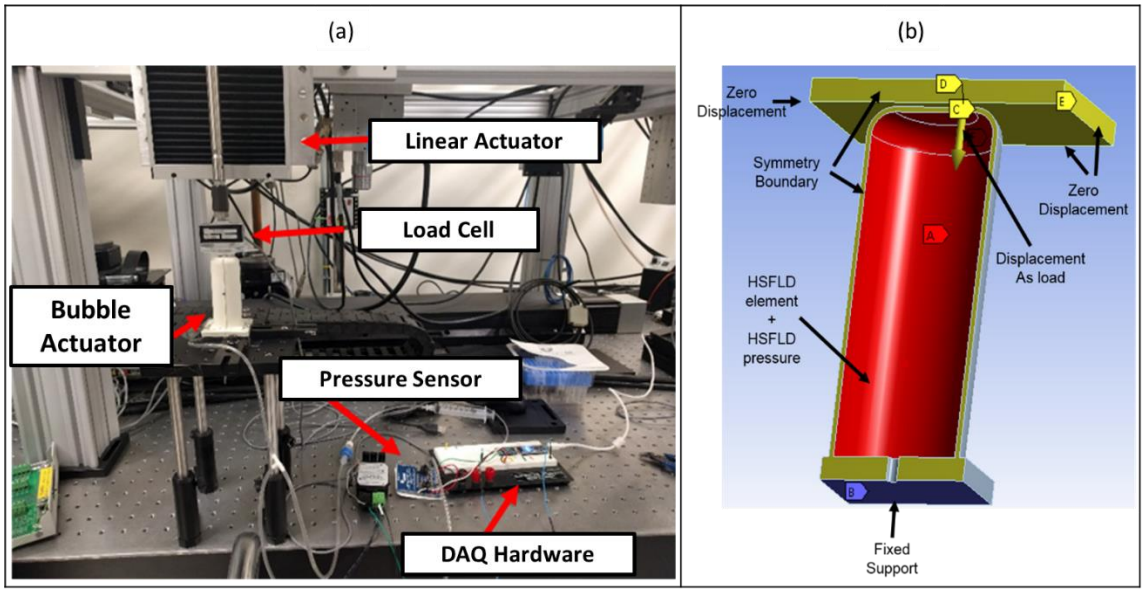

Figure 13 (a) Test setup to record and monitor internal pressure, interface force and deformation, (b) Schematic of conditions used for the FE model to simulate deformation of bubble actuator interacting with an external load.

- **Significant results:**

Developed and validated a simulation model which can predict the mechanical behavior of the actuators under loading conditions. This model will be used for simulating the entire seat cushion to predict interfaces between the seat cushion and user.

Free expansion experimental and simulation results

Fig. 14(a) and (b) show deformations of four named points TC, TR, MC, MR. Note that the deformation of BC and BR is insignificant in magnitude compared to the above four and thus excluded from the plots. The deformation results from three different samples are presented with circles representing mean deformations and length of error bars representing the standard deviation. Continuous solid lines represent the same deformations predicted by the simulation.

The two prominent modes of deformation are along the Y direction for TR, TC (TR-y, TC-y) and radial deformation for MR, MC (MR-z, MC-x). It is observed that experimental deformations follow the trend predicted by simulations very closely, albeit with an acceptable variation (TR-y) in some cases. The simulation predicts zero tangential motion for all the points due to ideal symmetric boundary conditions (x coordinate of MR, TR; z coordinate of MC, TC). During testing, the samples have non-zero deformation due to inherent asymmetry. The variations are also observed to be high across different samples due to the unavoidable non-uniformity in the manufacturing process. However the magnitude of such variations and deviations is insignificant compared to the major modes of deformation.

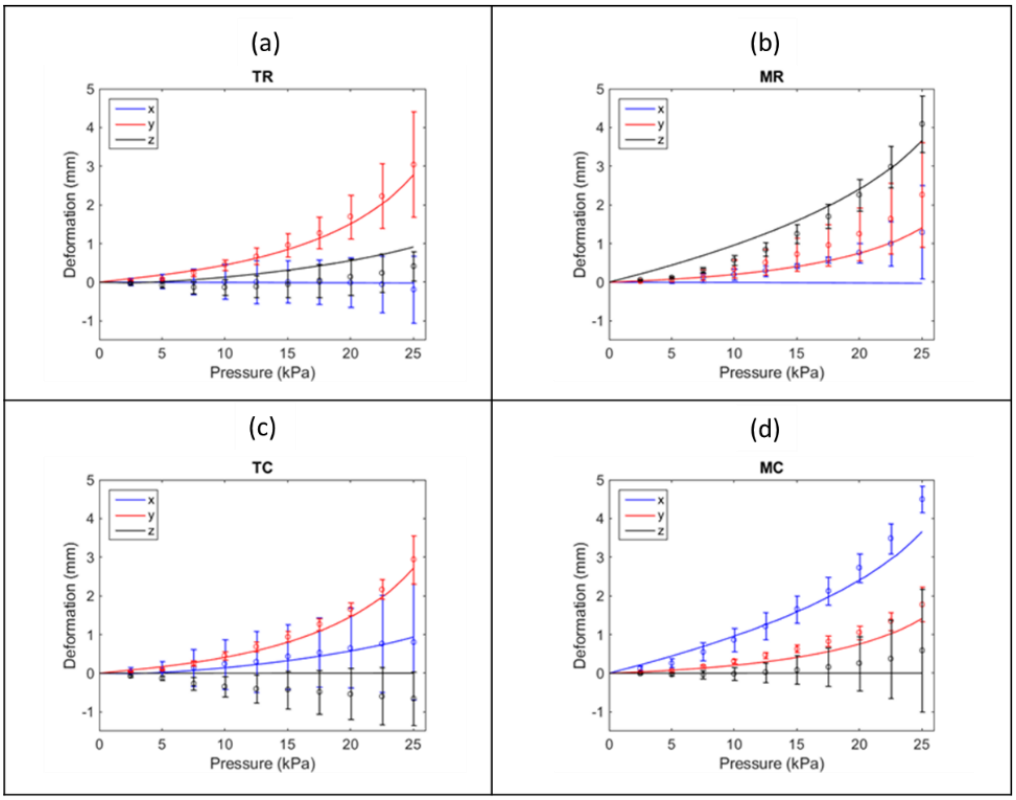

Figure 14 Plot of deformations of reference points across the pressure range from both experimental as well as simulation study for points (a)TR, (b)MR, (c)TC, and (d)MC.

Applied load experimental and simulation results

Figures 15(a) and (b) show plots of sensor measurements from the experiment compared with its simulated counterpart. Note that the sensors record data at a sampling rate of 100 – 130 Hz which makes experimental data continuous for all practical purposes. Due to the nature of asynchronous data collection, averaging measurements across different samples and even different trials with the sample does not yield any meaningful data. The plots from all three different samples follow the same trend to an acceptable degree. Data from one of the samples is presented in Figures 14(a) and (b).

The experiments consistently show that the bubble actuator buckles in the axial direction after a certain deformation in the Y direction. It is observed that this deformation limit increases with increasing initial inflation pressure. The maximum deformation limit corresponding to buckling is recorded from experiments and FE model is simulated until such limit. The plots from Fig. 15(a) show agreement between such simulated cases and their corresponding experimental results. Deviations from predicted behavior can be explained by manufacturing imperfections of the bubble actuator. The plots from Fig. 15(b) show a consistent linear relationship between internal pressure and interface force. The consistent deviation of the slope from their simulated counterparts shows the validity of the model with an acceptable tolerance.

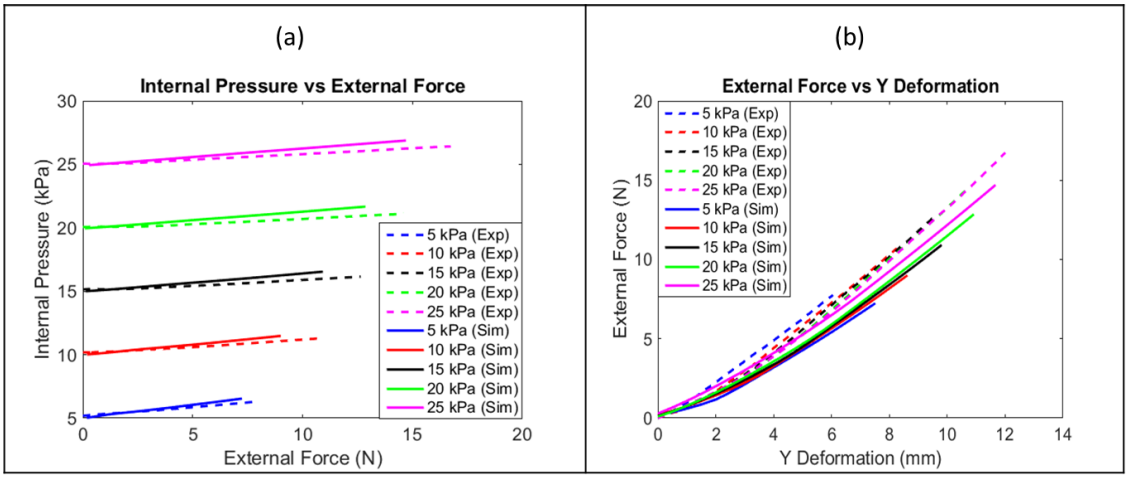

Figure 15 (a) Plot of external force vs Y deformation at various initial inflation pressures for both simulation and experimental study and (b) Plot of internal pressure vs external force at various initial inflation pressures for both simulation and experimental study.

Accomplishment #3: Design, assembly, and testing of pneumatic control system and electronics for 5x5 actuator test platform

- **Specific objectives:**

1) Develop the control unit to map and modulate the internal pressure of a 5x5 actuator array when subjected to an external load
2) Test the control unit for pressure modulation of each actuator to demonstrate pressure offloading and redistribution across the array

- **Major activities**:

1) Designed and developed benchtop control unit to verify the pressure modulation operation (Fig. 16). Assembled a benchtop based pneumatic control system to facilitate testing of pressure mapping and modulation capabilities. In order to accomplish this, a requirements analysis study was carried out to identify specific components including pressure sensors, solenoids, controller, pump, and a regulator. Using these components, circuits were designed for each of the modules and PCBs were developed to mount sensors, MOSFET switches, and solenoids. The operation of individual circuit modules was tested, after which the system was integrated as shown in Fig. 16. The integrated system was then tested to verify its operation and capability of modulating pressure.

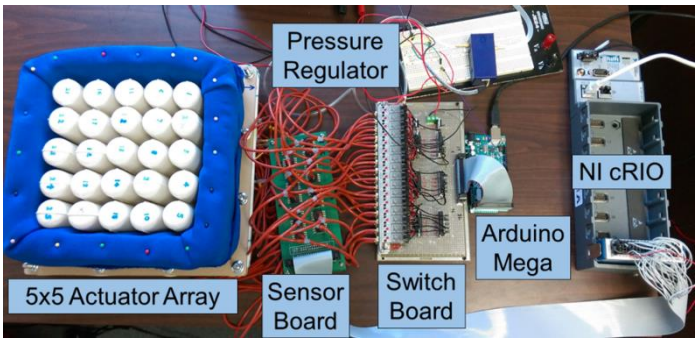

Figure 16 Benchtop control system with labeled components

2) Reorganized the pneumatic control unit to fit the system under the 5x5 bubble actuator prototype so that the final control unit can be fitted underneath the full automated seat cushion (Fig. 17). The benchtop based pneumatic control system was useful for the preliminary hardware test setup. In order reduce the size of the test system, the length of the air channels was reduced and the electronic components of the control unit were rearranged to fit under the 5x5 prototype, as shown in Fig. 17.

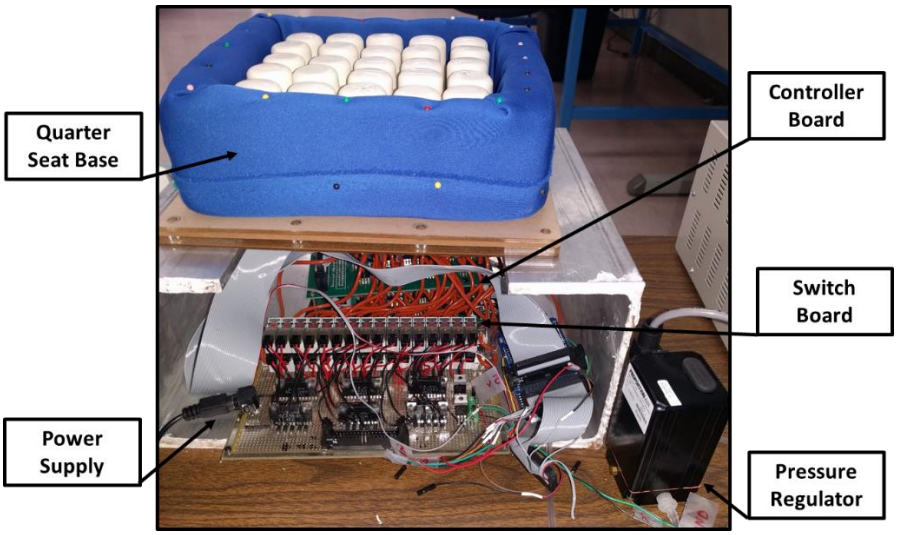

Figure 17 Reconfigured control system fitted underneath the 5x5 test platform

In this size reduction effort, the following specific activities were performed:

i. Implemented the input and output functionalities onto a single controller board: The features and capabilities of the previous system included separate devices for the input and output functions. Earlier, data acquisition from the pressure sensors was carried out by a NI cRIO-9074 chassis via a NI 9205 module while actuation was controlled by an Arduino microcontroller board. In order to reduce the size and weight of the system, both of these functions were integrated into a single Arduino microcontroller board.

ii. Integrated new hardware into the control system for better control of the pressure: The OEM-EP miniature pressure regulator has been replaced by the QPV1 from Proportion Air in order to overcome the irregularities and inconsistencies observed in the former regulator. A Bluetooth module has also been integrated into the system to wirelessly communicate with the GUI.

3) Developed a GUI to visualize internal actuator pressures and to modulate individual actuator pressures

i. The C# based GUI provides a functional layout of the relevant controls and user inputs for better ease-of-use. It depicts the location, number, and internal pressure of each bubble to match the quarter seat cushion layout and also displays a color coded map of internal pressure at the corresponding interface location. Furthermore, the GUI provides the user with options including the ability to record pressure datasets along with timestamps for further analysis. The interface provides the following capabilities: 1) set individual or all bubble actuators to a given pressure or edit pressure values 2) select mode of communication - Serial or Bluetooth 3) change unit of pressure between kPa or psi and 4) select mode of operation between a Default Mode (Run Once) or Continuous Readjustment Mode, as shown in Fig. 18.

ii. Integrated a selectable capability for Bluetooth communication: The system is now programmed to transfer actuator pressure data via Bluetooth to the GUI. This would make the connection between the GUI and the control system wireless and will ensure greater portability of the system.

4) Verified the controller's capability of pressure mapping, offloading, and redistribution by testing under applied load

• **Significant results:**

Control unit development

1) The use of a single controller board for both the input and output functionalities has decreased the weight and size of the control unit, making it easier to deploy and more reliable in its testing. Functionally, the updated controller design requires less time for its initial setup, starts the inflation process sooner, improves data acquisition rate, and reduces latency.
2) Produced a control unit capable of modulating the internal pressure of each actuator in a closed-loop manner. There are two modes of operation where the actuators can be operated to attain a set pressure. In the Default Mode of operation, each actuator or group of actuators are set to the given pressure profile in one run i.e. once the pressures are set in the actuators, any change in pressure due to movement will be reflected on the GUI but not further modulated. In the Continuous Readjustment Mode, each actuator or group of actuators are set to a given pressure profile in continuous runs. Once the pressures are set in the actuators, the system will continuously readjust to the set pressure profile to accommodate for changes due to motion of the user.

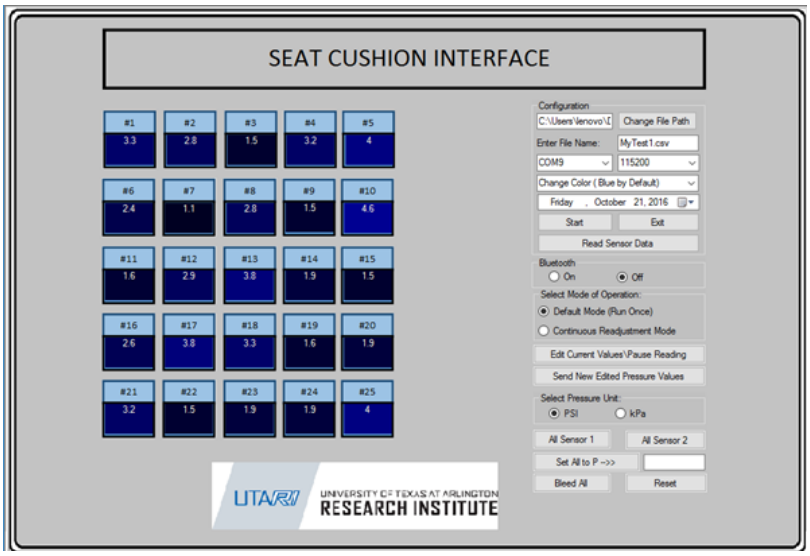

Figure 18 GUI demonstrating pressure mapping and modulation capabilities. The pressure changes in each of the actuators are reflected by a corresponding change in color for each of them.

GUI development and pressure modulation testing

1) Demonstrated the pressure mapping and modulation capability through the GUI as seen in Fig. 18. The GUI was integrated with the control system to facilitate visualization, modulation, and recording of actuator pressures. It gives a variety of options for the user to interact with the device.
2) Tested the pressure mapping capability of the system: An insert rod holder was attached to a spherical weight of 9.07 kg and was aligned perpendicular to the quarter seat base while allowing free movement along the axis normal to the quarter seat base, as shown in Fig. 19. The actuator array was subjected to an external normal load given by the spherical weight and the internal pressure across the actuator array was recorded from the GUI. A 2D pressure profile was generated using the recorded pressure data. Different pressure modulation schemes were applied while the weight remained on the actuator array, including pressure modulation of all actuators and select actuators.
   i. Pressure mapping capabilities of the system are demonstrated in Fig. 20. The test was carried out in three steps 1) The actuators were inflated to a uniform pressure 2) The weight was placed on the array 3) The resulting pressure map was recorded through the GUI.

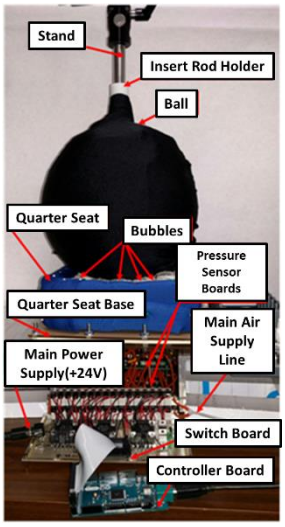

Figure 19 Test setup for pressure mapping and modulation capabilities

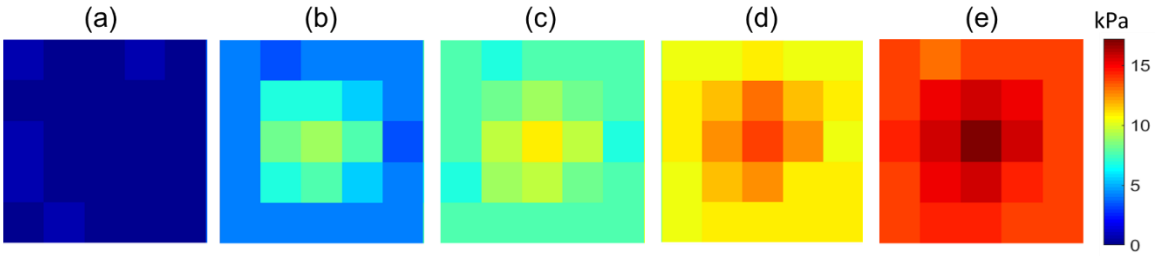

Figure 20 The internal pressure of all actuators are plotted when the weight is placed at the center for different inflation pressures, (a) before inflation and without a spherical weight; (b) all actuators are inflated at 3.5kPa; (c) all actuators are inflated at 7kPa; (d) all actuators are inflated at 10.5kPa; (e) all actuators are inflated at 14kPa

ii. Pressure mapping and modulation over all actuators is demonstrated in Fig. 21. The test was carried out in three steps: 1) The actuators are initially at atmospheric pressure 2) The spherical weight is placed upon the array and the pressure map is captured, as seen in Fig. 21(a) 3) The pressure across the array is set to differing set values of 5.5kPa, 3.45kPa, and 1.35kPa sequentially. This demonstrates the capability to uniformly redistribute pressure across the array. Furthermore, while reducing the pressure of all actuators, the contact area between the spherical weight and the actuator array is increased which is critical for reducing shear forces during seat cushion operation.

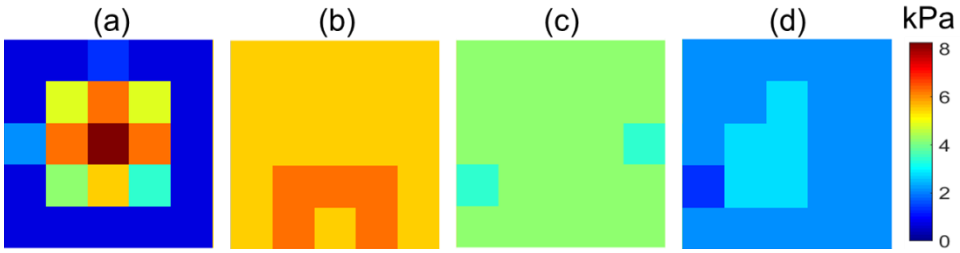

Figure 21 (a) Initial pressure map with the spherical weight placed at the center of the actuator array; (b) equalized pressure of all actuators to 5.5kPa; (c) equalized the pressure of all actuator to 3.45kPa; (d) equalized the pressure of all actuator to 1.35kPa.

iii. Pressure mapping and modulation over selective actuators is demonstrated in Fig. 22. Using similar conditions as the previous test, an initial pressure map was obtained as shown in Fig. 22(a). Only the pressure of the central nine actuators was reduced in a step by step fashion until a more uniform pressure distribution within those nine actuators was achieved.

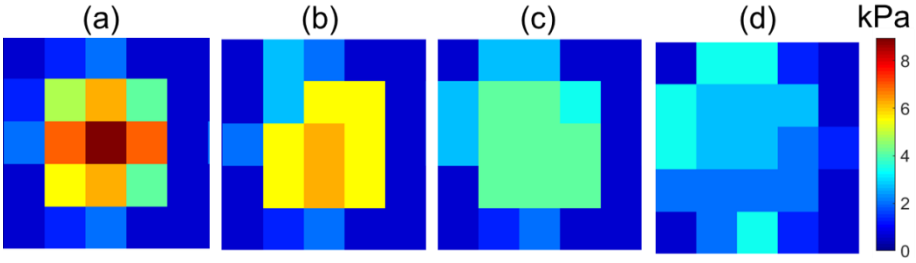

Figure 22 (a) Initial pressure map with the spherical weight placed at the center of the actuator array; (b) equalized the pressure of the center nine actuator to 5.5kPa; (c) equalize the pressure of the center nine actuator to 3.45kPa; (d) equalize the pressure of the center nine actuators to 1.35kPa

iv. The pressure offloading and redistribution capability is demonstrated in Fig. 23. The initial pressure map was obtained by placing the weight on the actuator array (Fig. 23(a)), the internal pressure of the central five actuators was reduced to zero gauge pressure for offloading (Fig. 23(b)), and the pressure of all remaining actuators was equalized to 3.5kPa to redistribute the pressure among other actuators (Fig. 23(c)).

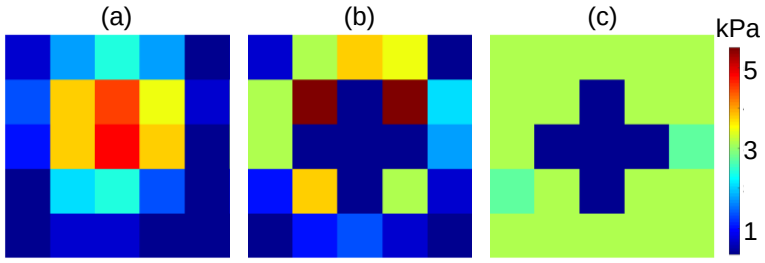

Figure 23 (a) Initial pressure map with the spherical weight placed at the center of the actuator array, (b) updated pressure map when the central five actuators are deflated, (c) equalized pressure to an average value of all remaining actuators

Accomplishments related to Aim 2: Conduct numerical and experimental studies on interface pressure and shear forces using an anthropomorphic model to develop a control algorithm.

Accomplishment #5: Development of automated control software to test pressure modulating algorithms for 5x5 actuator test platform

- **Specific objectives:**

1) Develop a comprehensive software suite for controlling the test actuator platform through a desktop computer
2) Automate the control of internal pressures with closed loop feedback control using the developed software solutions.

- **Major activities**:

1) The control problem is broken into two steps and a decentralized approach is taken to achieve the commanded pressures. The inner loop implemented on an Arduino MEGA 2560 microcontroller is responsible for monitoring the pressure values as well as operating the valves and proportional air regulator to maintain a given target pressure map. The microcontroller transmits the current pressure map to the computer for display and receives the target pressure map for inner loop control. The outer loop running on a desktop computer houses the algorithm to synthesize a target pressure map from the current pressure map. The desktop application displays the received pressure map as well as transmits a target pressure map. Decoupling of the control problem into inner and outer loops provides standalone performance guarantees in absence of the outer loop and flexibility for implementing the outer loop on various platforms (Windows, Linux, Mac, Android, IPhone). Similarly the inner loop can be implemented on any other embedded computing platform.
2) The program for Arduino microcontroller is written in Arduino IDE and is designed to run as a standalone unit even in absence of a desktop application. The code is also optimized to ensure maximum data rate while keeping memory usage low (2%) which ensures stable operation. The current pressure map is sent as an array of 10-bit values as read by 10-bit ADCs on MuxShield attachment of Arduino. Note that the code also incorporates flexible interface or easy access through any serial terminal and retrieval of diagnostic information.
3) The desktop application is designed to read the serial packets sent by the Arduino code and display the information in a matrix form as well as a contour plot. The application is developed using MATLAB's GUIDE API for access to matrix manipulation methods and fast deployment solutions. It can be compiled into an application for any platform (Windows, Linux or Mac). The interface also displays pertinent diagnostic information.
4) The communication architecture is established for efficient and error free data exchange between the microcontroller and the desktop computer.
5) Automatic operation of newer automated software suite was verified by replicating previously conducted pressure redistribution tests which were manually performed.

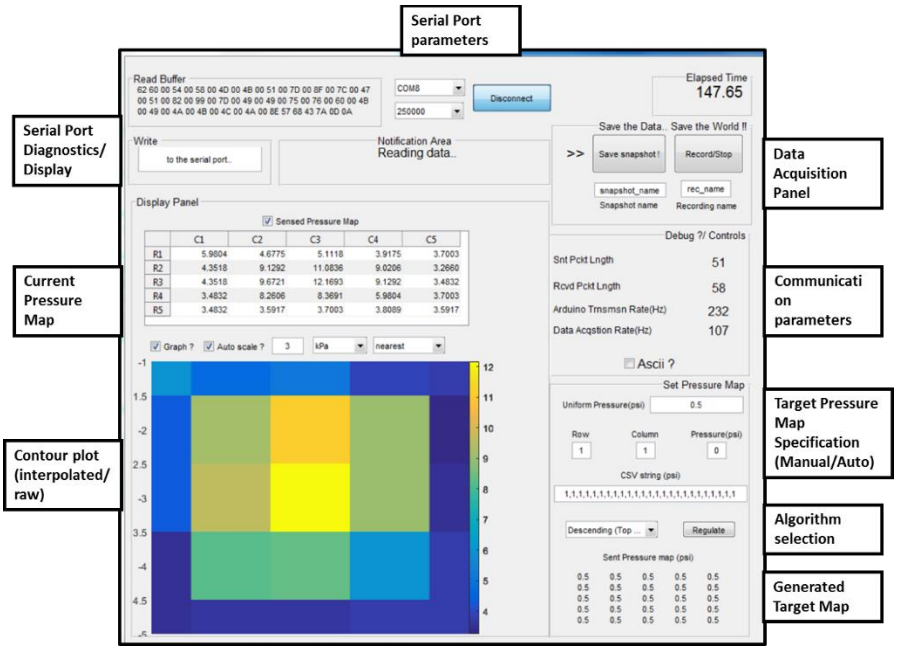

Figure 24 MATLAB based automated control system desktop application

6) The setup uses only one proportional air controller to control air pressure in 25 different actuator volumes. Simultaneous and thus more efficient method to approach the given target pressure map with two novel algorithms for inner loop control have been formulated.

Bottom-up:

a) Sort the actuators by target pressure in ascending order.
b) Starting with the lowest as target pressure on the proportional air controller, all the valves are opened.
c) As the lowest pressure actuator reaches its target, close the corresponding valve.
d) Set the next lowest as target pressure on the proportional air controller.
e) Repeat steps (c) and (d) until all the actuators are exhausted.

Top-down:

a) Sort the actuators by target pressure in descending order.
b) Starting with the highest pressure actuator as target pressure on the proportional air controller, all the valves are opened.
c) As the highest pressure actuator reaches its target, close the corresponding valve.
d) Set the next highest as target pressure on the proportional air controller.
e) Repeat steps (c) and (d) until all the actuators are exhausted.

Bottom-up tends to be more efficient while inflating the actuators from atmospheric pressure. Top-down tends to be more efficient when offloading higher pressure areas without deflating the entire array of actuators.

7) An outer loop control algorithm is developed to relieve high pressure points from the current pressure map and redistribute it among other actuators with lower pressure. Such algorithms synthesize a target pressure map from current pressure map and are by no means unique. No claims of stability or performance can be made at this point due to unavailability of a dynamic model. The control algorithms are inspired by an intuitive line of reasoning and can be easily implemented into the application (outer loop). One such algorithm is implemented with successful control. It is assumed that the sum of pressures is a constant among both current as well as target pressure maps.

a) Find the maximum and minimum pressure of current pressure map.

b) Set an adjustable threshold $= \min \overline{P} + \delta(\max \overline{P} - \min \overline{P})$ where δ is parameter which determines the distance of pressure relief from the maximum pressure point ($0 < \delta < 1$).
c) Set all the actuators with pressure higher than the threshold to 0 kPa.
d) Evenly distribute the relieved pressure into rest of the actuators.

• **Significant results:**

Sensor and communication specifications

1) Sensor specifications: The pressure sensors (MPX5100G) have analogue outputs with operational range of 0 to 100 kPa. The 10-bit resolution of ADCs determines the operational resolution of the sensors (0.09 kPa). The proportional pressure regulator requires an analogue voltage to control the pressure in the range of 0 to 103 kPa. A low pass filtered digital PWM signal from Arduino's 8-bit DAC determines the operational resolution of the pressure regulator (0.4 kPa).
2) Communication specifications: Legacy serial ports via USB are used to establish communication between the inner and outer loops at a baud rate of 250,000 bits/second. The inner loop has two modes of output for diagnostic purposes (ASCII and binary). The binary mode is implemented to allow faster and more efficient communication using a serial interface. The inner loop as well as the outer loop are timed and instantaneous speed is recorded for diagnostic purposes. The inner loop on the Arduino runs at around 230 Hz in binary mode and 60 Hz in ASCII mode (with loss of resolution). The speed of inner loop determines the maximum outer loop speed. The outer loop implemented on MATLAB runs at 170 Hz with a display refresh rate of 10 Hz. The outer loop rate which determines time resolution of data capture can be pushed to maximum if display refresh rate is sacrificed or by running it on a better desktop processor. At this point, both the rates are well within acceptable limits for seat cushion operation as well as development.

Validation of automated control algorithms for pressure modulation

Note for pressure plots: The plots in the upper row show raw data captured from the 5x5 array, while the plots below show the data interpolated onto a finer (10x) mesh using biquadratic basis functions. The interpolated distribution is only used for display. All computations are performed on raw data only.

i. Pressure display and data capture: Pressure mapping and display are shown at various initial uniform inflation pressures across all actuators. A spherical weight of 9.07 Kg is lowered vertically onto the center of the prototype. The pressure maps from Fig. 25 show the pressure increase in an otherwise uniform distribution occurs more towards the center where actuators deform more to accommodate the geometry of the spherical weight.

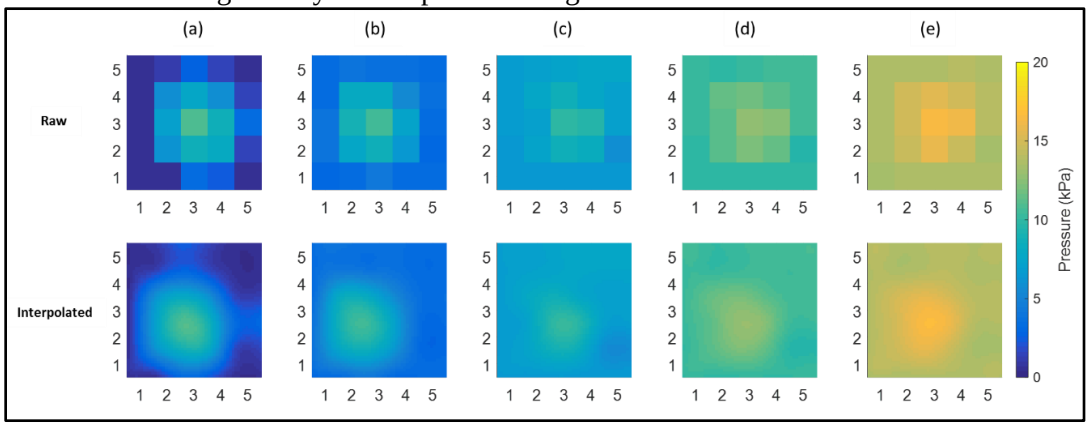

Figure 25 The sensed pressure map with the spherical weight placed at the center of the actuator array inflated to a uniform gauge pressure of (a) 0 kPa, (b) 3.5 kPa, (c) 7 kPa, (d) 10.5 kPa, (e) 14 kPa.

ii. Automatic pressure regulation with a uniform target distribution: Initially the spherical weight is placed at the center of 5x5 array held at 0 kPa. Then various uniform target pressures are specified by the outer loop (7 kPa, 5.5 kPa, 3.45 kPa, 1.35 kPa). The pressure maps from Fig. 26 show that all the given pressure distributions are reached with minimal non-uniformities. Note that the capability to regulate to a certain uniform target pressure diminishes as the target pressure decreases. There is a certain minimum pressure determined by the weight of the object placed. For example, a 0 psi pressure distribution would mean there is no weight placed on the seat cushion.

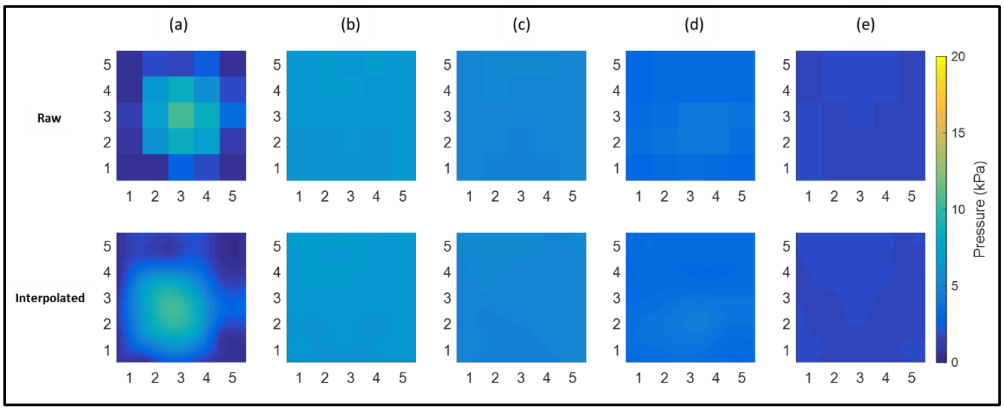

Figure 26 (a)The sensed pressure map with the spherical weight placed at the center of the actuator array inflated to a uniform gauge pressure of 0 kPa, (b) The sensed pressure map with the spherical weight after the pressure is uniformly regulated to 7 kPa, (c) 5.5 kPa, (a) 3.45 kPa, (e) 1.35 kPa.

iii. Automatic pressure regulation using the presented algorithm: Initially the spherical weight is placed at the center of 5x5 array held at 0 kPa. Then the current pressure distribution is read by the outer loop and a target pressure map is synthesized using the presented algorithm for outer loop. The distributions show identical performance while using both top-down and bottom-up algorithms. The point of maximum pressure is offloaded to 0 kPa and the surrounding areas bear more pressure which results in deformation of the seat cushion to accommodate the geometry of the spherical weight. This also results in more contact surface as the weight lowers into the seat cushion. Note that there is a distinction between pressure maps read while all the valves are closed and while they are controlled by the algorithm for pressure redistribution. The actuator internal pressure is directly proportional to the interface pressure (as validated by our previous bench-top experiments) only when the weight is applied after all the valves are closed.

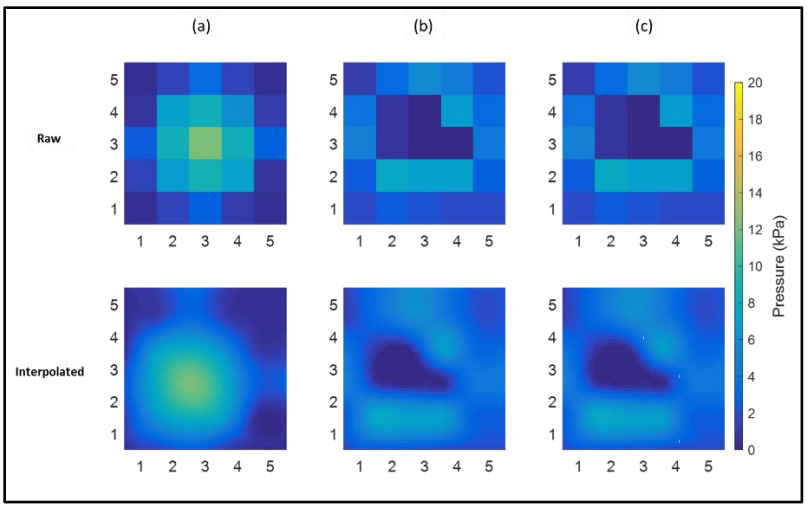

Figure 27 The sensed pressure map with the spherical weight placed at the center of the actuator array inflated to a uniform gauge pressure of 0 kPa, (b) The sensed pressure map with the spherical weight regulated by the outlined algorithm for the outer loop, with Top-down algorithm for inner loop, (c) with Bottom-up algorithm for inner loop.

Accomplishment #6 (U Pitt): Finalized the design of the sensorized anthropomorphic model

- **Specific objectives:**

1) Conceptual design of a sensorized anthropomorphic model capable of measuring both interface shear and pressure characteristics of the wheelchair seat cushions

- **Major activities**:

1) Literature review of current state of art of the wheelchair seat cushion test standards and cushion loading indenter being used.
2) Formed the design criteria for the sensorized anthropomorphic model based on the ISO 16840-2 standard, literature review and design meetings.
3) Conceptualized drawing of a sensorized anthropomorphic model with strain gauges at proximal left/right buttock (PLB/PRB), distal left/right buttock (DLB/DRB), left/right trochanter (LT/RT), left/right ischial tuberosity (LIT/RIT), and sacral region (SR) as shown in Figure 28(a).
4) Designed the initial sensorized anthropomorphic model based on the conceptualized drawing shown in Figure 28(b).

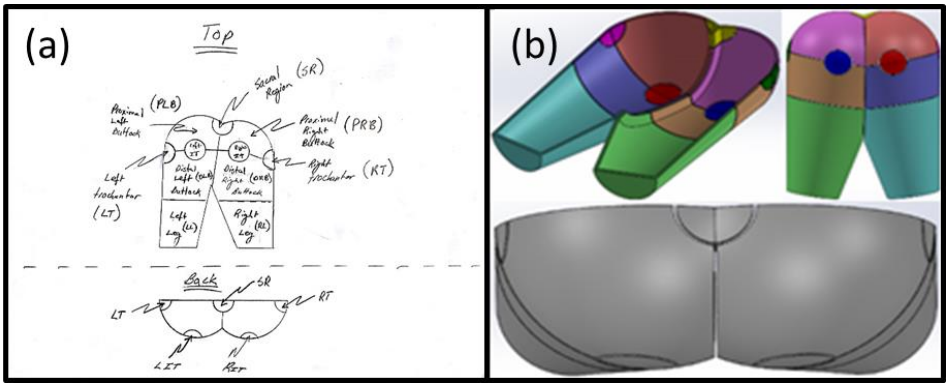

Figure 28 (a) The top-down view and anterior-posterior view of conceptualized drawing of the sensorized anthropomorphic model based on standard, literature review, and design meetings. (b) CAD model of the conceptualized design. The left and right buttock are symmetric but they will be fabricated separately. In addition, they could be attached together with offset on top-down plane, or with gap between them to accommodate patients with different anatomical shapes.

Accomplishment #7: Finalized the design of the sensorized anthropomorphic model

- **Specific objectives:**

1) Fabricated a piece of the designed buttock and tested the sensors to measure forces.

- **Major activities**:

1) A 250UW general purpose strain gages from Vishay Precision Group was selected. The overall gage dimension is 11.43mm by 4.57mm with gage size 6.35mm by 4.57mm.
2) Fabricated a piece of the designed model of the buttock for which forces and torques of all three axis needed to be calculated.
3) Attached the strain gage to the fabricated piece, designed the electrical circuit to read the gages as shown in Figure 29(a).
4) Developed the model to calculate the forces regarding to the deformation of gage change as shown in Figure 29(b).
5) Test the strain gage attached to the fabricated piece with various load as shown in Figure 30(a).
6) The data collected from the strain gage after calibration as shown in Figure 30(b).

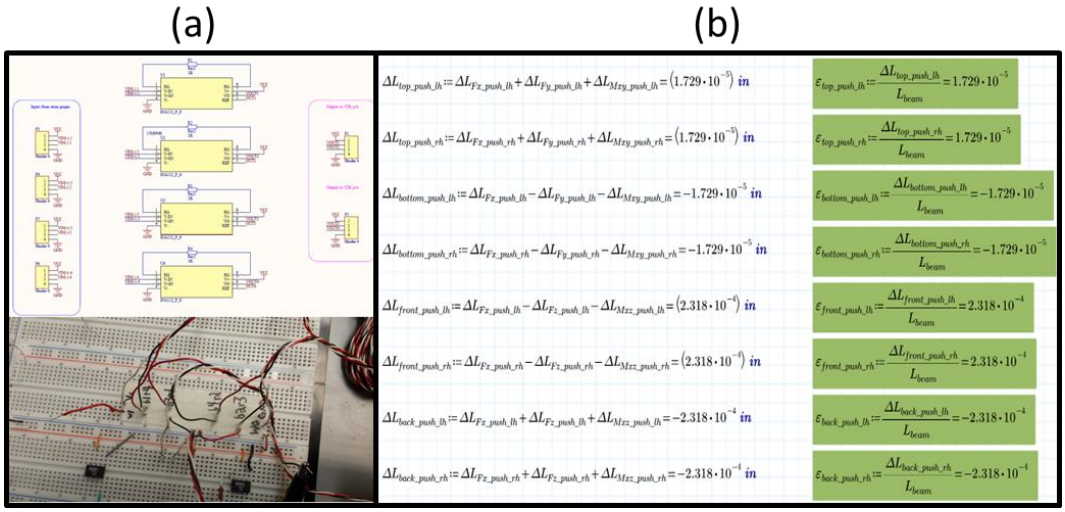

Figure 29 (a) The circuit board designed to collect data from strain gage. (b) The mathematical model developed to calculate the forces from strain gage.

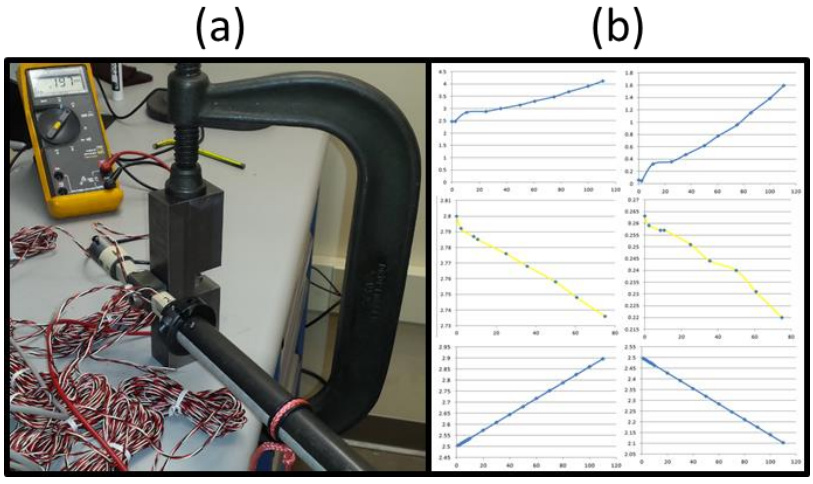

Figure 30 (a) The fabricated piece of the buttock instrumented with the strain gage was tested and calibrated. (b) Plots of the data collected from the strain gage.

Accomplishment #8: Finalized the design of the sensorized anthropomorphic model

- **Specific objectives:**

1) Finalize the sensory system to measure pressure and shear force distribution simultaneously.

- **Major activities**:

1) Being that industrial/competitive load cells do not typically measure both shear and compression/tension, but instead measure one and isolate the other, we had excluded the possibility of using commercial load cells for this application, and have designed custom sensors.
2) A design using an S-beam on top of a hollow column had been tested as shown Figure 31(a). This design used a full-bridge arrangement of dual-pattern gauges (Tee rosettes) on the hollow column, creating two full-bridges that allowed us to measure anterior-posterior shear and mediolateral shear. We would need to replicate these transducer elements (each has four, full bridges for a total of 8 rosettes per column + S-beam pair) for each section of the posterior designed in previous report.
3) For 13 sections having one transducer each, this would bring us to a total of 52 gauges (or 26 Tee-rosette patterns). They are available for Titanium from HBM in 350 ohm resistance in the following sizes (a, b, c are in mm):
4) A system diagram for basic S-beam-like design had been developed and sketched out as shown in Figure 31(b). A usable pattern and geometry of strain gauges were also determined.

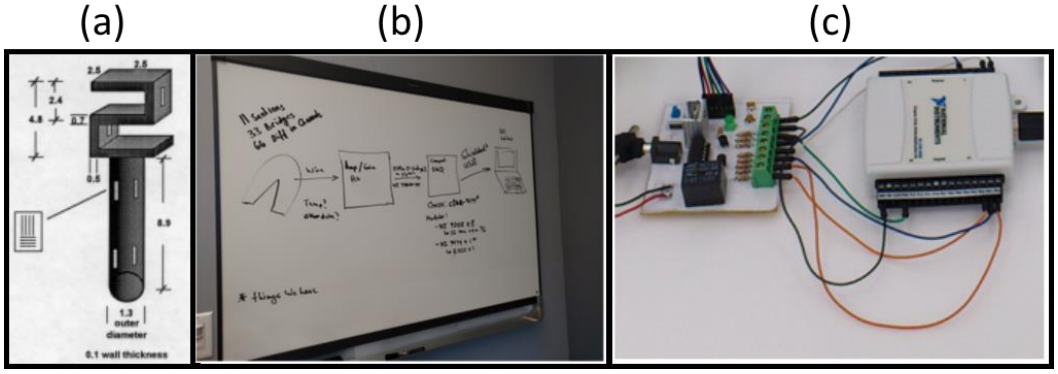

Figure 31 (a) The schematic design of the transducer consists of a hollow column with an S-shaped cantilever; both will be machined from Titanium. (b) The system diagram for electrical hardware and data collection. (c) The purchased multichannel NI 9205 32-Ch ±200 mV to ±10 V, 16-Bit, 250 kS/s Analog Input Module and NI 9474 24 V, Sourcing Digital Output, 8 Ch Module

Accomplishment #9: Fabrication and validation non-sensorized anthropomorphic model with identical dimensions and shape to the sensorized model had been fabricated and assessed for the pressure measurability. A test beam for the sensorized model had been modeled, simulated and fabricated to prove the approach. We are behind the schedule on fabrication the complete sensorized anthropomorphic model. We will have the sensorized anthropomorphic model fabricated and validated by end of fiscal year of 2016)

- **Specific objectives:**

1) Fabrication and validation of the sensorized anthropomorphic model.

- **Major activities**:

1) A first generation anthropomorphic model had been designed and fabricated as shown in Figure 32(a).
2) The required data acquisition hardware had been purchased: The DAQ NI 6128-USB and the NI-9174 Analog Input modules, NI-9474 DIO input, and an NI cDAQ-9174 chassis, which connects with the LabView computer via USB (as shown in Figure 32(b)).
3) The pressure measurability of the model has been evaluated with various commercial cushions. An Invacare cushion, permobil cushion and pride cushion (Figure 32(c)) were evaluated with the MTS

machine (Figure 32(d)). The pressure measurability as shown in Figure 33 was tested with very good consistency with previous test data available for those cushions.

4) FEA analysis and modeling of test beam: The test beam composed two parts linked together, an S-shape part and a circular column as shown in Figure 34(a). The following finite element analysis (FEA) was performed to examine the design: natural frequency, strain and stress under pure compression, pure shear and combination of both compression and shear (Figure 34(b)). The test beam CAD model was meshed to 422735 elements (Figure 34(c)). Radius of 0.01" was added on the corner to alleviate the stress concentration from the sharp corners. The corners were refined in order to provide better transition. The boundary conditions were applied as following. The bottom face of the beam design was fixed. The compression and shear forces were applied on the top of the beam. As there will be 11 test beams placed in the anthropomorphic model, the compression force applied on each test beam (23 lbs) was assumed as the average of the human weight (250 lbs) and the shear force (12 lbs) was assumed as the half of the compression force. The materials used in for the simulation were Aluminum 1060 alloy, Titanium Commercially Pure CP-Ti UNS R50400, and Alloy Steel. The natural frequency was analyzed with rigid fixture on the top of the beam and the bottom was freely moved as shown in Figure 34(d). Strain and stress analysis was examined to simulate the response on the strain gauges. The strain gauges are placed on the outside and inside of the S-shape part and three pair on the column to measure the vertical deformation as shown in Figure 34(e). Results of the strain analysis was shown in Table 2.

Table 2 Results of strain analysis

Material	Aluminum	Titanium	Steel
Mode 1 Frequency (Hz)	226.05	236.04	254.35
Mode 2 Frequency (Hz)	333.51	344.65	380.09
Mode 3 Frequency (Hz)	818.21	818.4	881.28
Mode 4 Frequency (Hz)	1188.6	1146.6	1274.8
Mode 5 Frequency (Hz)	1979.6	2006.2	2224.5
Pure Compression Strain	2.417×10^{-4} (Outside) -2.764×10^{-4} (Inside) -1.215×10^{-5} (Column)	1.587×10^{-4} (Outside) -1.815×10^{-4} (Inside) -8.005×10^{-6} (Column)	7.948×10^{-5} (Outside) -9.086×10^{-5} (Inside) -4.004×10^{-6} (Column)
Pure Shear Strain	-3.899×10^{-4} (Outside) -1.620×10^{-4} (Inside) 1.989×10^{-4} (Column) -1.028×10^{-4} (Column)	-2.842×10^{-4} (Outside) -1.064×10^{-4} (Inside) 1.307×10^{-4} (Column) -6.754×10^{-5} (Column)	-1.422×10^{-4} (Outside) -5.327×10^{-5} (Inside) 6.532×10^{-5} (Column) -3.376×10^{-5} (Column)
Shear and Compression	-1.909×10^{-4} (Outside) -4.384×10^{-4} (Inside) 1.866×10^{-4} (Column) -1.150×10^{-4} (Column)	-1.254×10^{-4} (Outside) -2.880×10^{-4} (Inside) 1.226×10^{-4} (Column) -7.556×10^{-5} (Column)	-6.275×10^{-5} (Outside) -1.441×10^{-4} (Inside) 6.129×10^{-5} (Column) -3.776×10^{-5} (Column)

The natural frequency results showed that the mode 1 frequency was 226-254Hz, which is much higher than the cushion testing system. Therefore, the "ringing" effect can be minimized. The strains at the strain gauges install location was retrieved to compare the differences between materials. The aluminum has the largest strain under all three conditions of force. The steel was the smallest and the titanium was in between. Under the pure compression condition, the strains on the outside and inside of the S-shape was about 20 times larger than the strain on the column. In the pure shear force condition, strain on one side of the column was twice larger than the other side. This was because the three pairs of strain gauges were install with 60 degrees of angle. The S-shape also found strain about twice larger than the strain on the column. When applying the shear and compression, the column strains reduced about 8% but the strain on the outside and inside S-shape were the summation of the strain found under

the pure compression and pure shear conditions. The deformation of the beam was within 0.2mm, which is acceptable in the cushion testing. An optimization on the dimensions of the S-shape thickness and the column thickness was performed to achieve the goal of maximize the strain gauge reading but retain the load cell under safety factor of 1.5. In this way, the strain gauge would have the optimized deformation, which increase the sensitivity. The range of S-shape thickness for optimization was 0.3" to 1" and the thickness of the column was ranging between 0.01" and 0.1". The optimized solution found was 1" S-shape thickness and 0.01" column thickness. In summary, the beam in the anthropomorphic model was designed and validated its dynamic and static response using the finite element analysis. In addition, design optimization was performed to achieve better sensitivity to the strain gauges.

5) Given the complexity of the full sensorized model (11 segments of the butt with six sensor on each segments of 66 sensors in total), we decided to make sure it worked before fabricate the full model. Thus a test beam had been fabricated and instrumented with strain gauge (Figure 35) to test the design and to be used for preliminary validation.

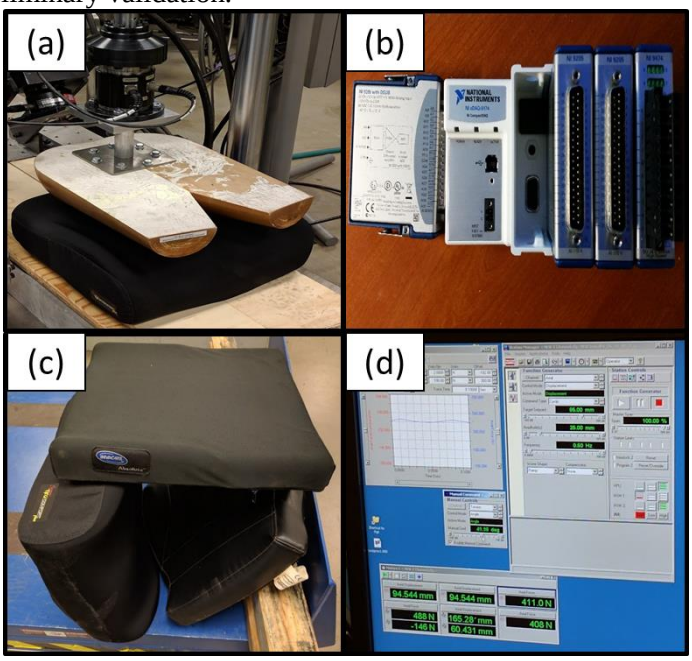

Figure 32 (a) The anthropomorphic model had been designed and fabricated to test pressure measurability (b) The purchased multichannel NI 9205 32-Ch ±200 mV to ±10 V, 16-Bit, 250 kS/s Analog Input Module and NI 9474 24 V, Sourcing Digital Output, 8 Ch Module (c) The three commercial cushions been tested with the anthropomorphic model Gen 1. (d) The MTS machine display of the test parameters and set-up

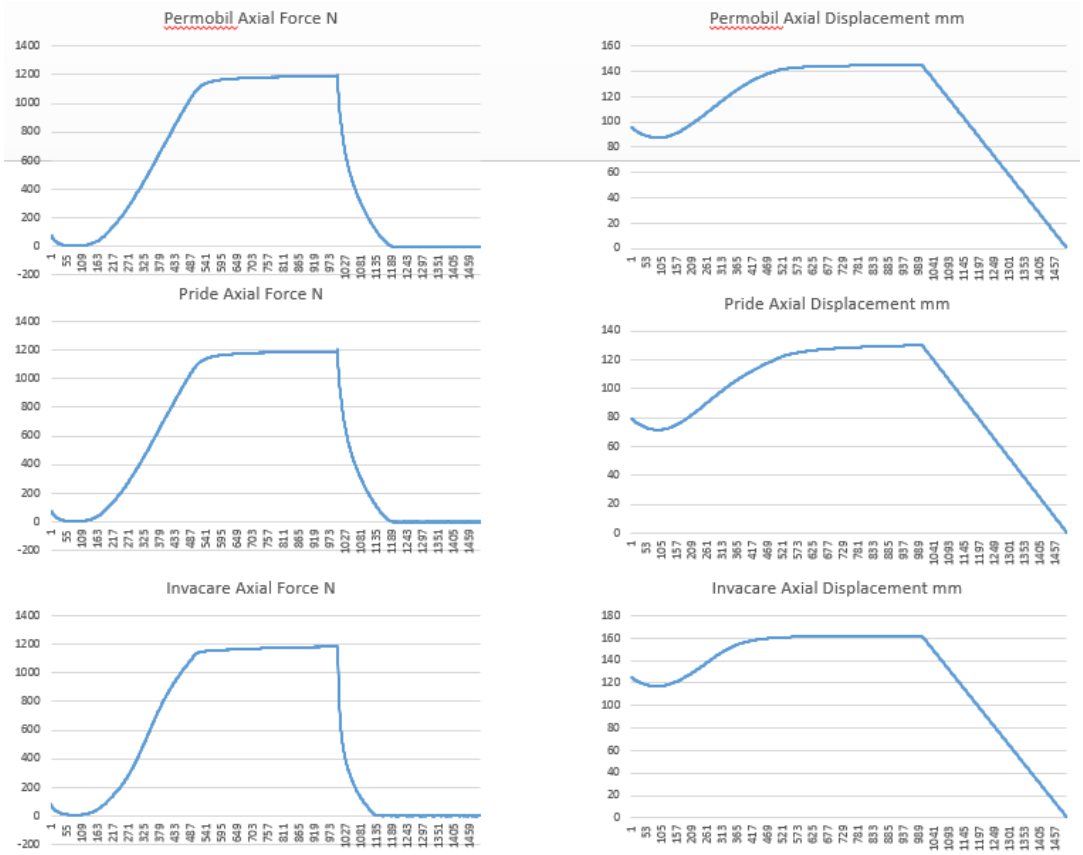

Figure 33 The test results showed very good pressure measurability of the anthropomorphic model

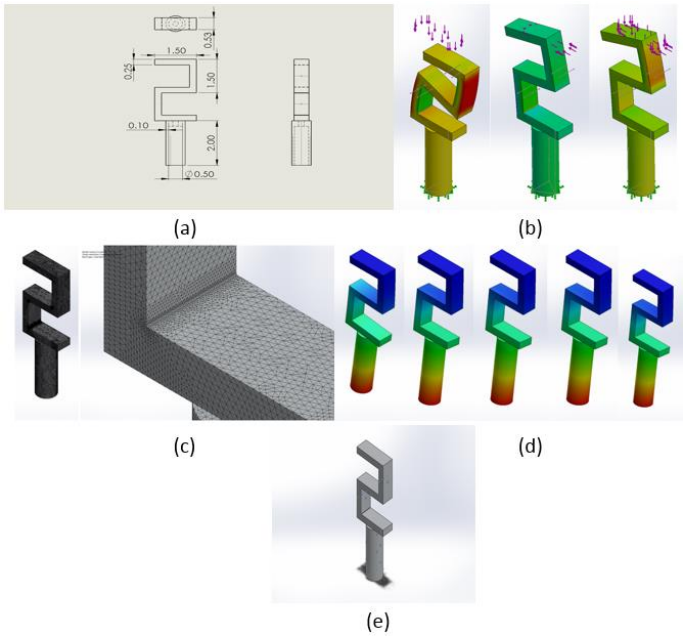

Figure 34 (a) the beam design; (b) Three types of simulated force conditions: from left to right, pure compression, pure shear, combination of compression and shear; (c) the meshed model of the test beam design; (d) the five modes of the natural resonance response (1 to 5 from left to right); (e) strain gauges' location.

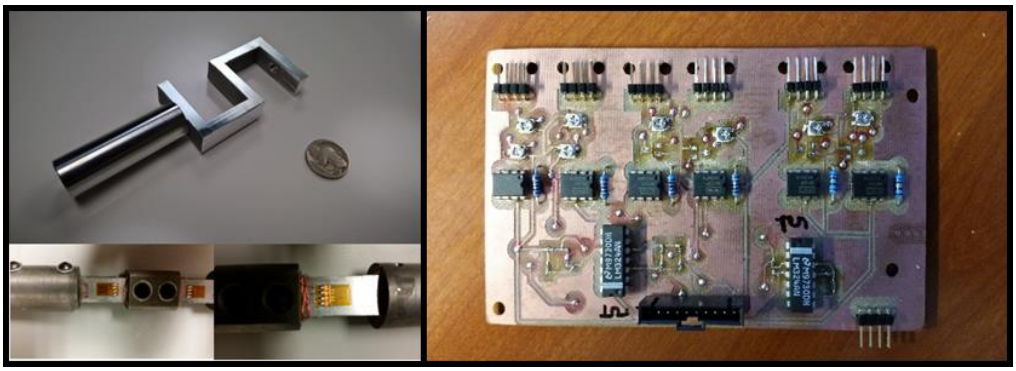

Figure 35 The fabricated test beam with strain gauge attached and the printed circuit board with amplifiers and A/Ds for the test beam.

- **What opportunities for training and professional development has the project provided?**

In addition to supporting full time engineers and research scientists, this project has provided learning opportunities for 6 student interns. The project offers practical engineering experience in developing real world solutions, which cannot be learned in a traditional classroom environment. This includes polymer molding, process development, ISO testing standards, etc. Furthermore, the project exposes them to medical device requirements in product research and development.

- **How were the results disseminated to communities of interest?**

The results have not been published at this time; however, up to two manuscripts are planned for submission before the next annual report.

- **What do you plan to do during the next reporting period to accomplish the goals?**

1) Complete seat cushion prototype with integrated control unit and graphical user interface
2) Algorithms to identify anatomical features, recognize vulnerable areas based on pressure profiles and perform the pressure relief strategies
3) Investigate the performance of various control algorithms to offload and redistribute pressure under changing loading conditions.
4) Perform finite element modeling of seat cushion with anthropomorphic model to simulate interactions of a person on a cushion.
5) Test seat cushion using sensorized anthropomorphic model.

4 IMPACT

- **What was the impact on the development of the principal discipline(s) of the project?**

1) The development of this pressure modulating seat cushion will advance the standard of care for pressure ulcer prevention, especially for spinal cord injury individuals.
2) This seat cushion enables longitudinal data collection of pressure distribution of a seated person which would enable retrospective analysis and improvement of preventative clinical protocols.
3) This technology can also be extended to pressure offloading and redistributing beds for patients in hospital settings and long term care facilities.

- **What was the impact on other disciplines**

Pressure modulating interfaces can be applied to other industries including defense and transportation. For instance, armored vehicles and fighter planes see passengers seated for extended periods of time in a confined setting and may be subject to constant vibration. Another example could extend to seat cushioning for international passenger flights and long distance commercial trucking.

- **What was the impact on technology transfer?**

Before this project began, a PCT patent was filed with the Office of Technology Management at UTA. Currently, this patent is under US Nationalization review.

- **What was the impact on society beyond science and technology?**

A potential effect on the quality of life for the patients relying on wheelchairs is expected. If such a device is achieved and generates sufficient interest, commercial applications and production could lead to the generation of a new branch of the medical seat cushion industry.

5 CHANGES/PROBLEMS

- **Changes in approach and reasons for change**

No changes have been made in the overall approach.

- **Actual or anticipated problems or delays and actions or plans to resolve them**

The sensorized anthropomorphic model fabrication has been delayed until ISO testing of multiple seat cushions using a non-sensorized model with identical dimensions and shape has been completed to assess its pressure measurability. This milestone will be completed by the next quarterly report in 2016.

- **Changes that had a significant impact on expenditures**

No significant changes in expenditures.

- **Significant changes in use or care of human subjects, vertebrate animals, biohazards, and/or select agents**

No human subjects, vertebrate animals, biohazards, and/or select agents are used in this study.

6 PRODUCTS

1) Cylindrical and rectangular bubble actuators for interface pressure offloading, modulation, and weight bearing
2) FE model of cylindrical actuators
3) GUI for seat cushion pressure mapping and controlling.
4) Control architecture for closed loop pressure modulation
5) S-shaped beam for shear and pressure transduction
6) Non-sensorized anthropomorphic model for seat cushion testing

7 PARTICIPANTS & OTHER COLLABORATING ORGANIZATIONS

- **What individuals have worked on the project?**

University of Texas at Arlington Participants

Name:	Muthu Wijesundara
Project Role:	PI
Researcher Identifier:	
Nearest person month worked:	1.2 (For the first year of the project)
Contribution to Project:	Provide the guidance of test setup design and configuration
Funding Support:	

Name:	Wei Carrigan
Project Role:	Researcher
Researcher Identifier:	
Nearest person month worked:	2.0 (For the first year of the project)
Contribution to Project:	Built test setup, fabricated air cells, and performed test and data analysis
Funding Support:	

Name:	Mahdi Haghshenas-Jaryani
Project Role:	Researcher
Researcher Identifier:	
Nearest person month worked:	2.4 (For the first year of the project)
Contribution to Project:	Performed numerical analysis and optimization of the air cell for the cushion
Funding Support:	

Name:	Charu Pande
Project Role:	Researcher
Researcher Identifier:	
Nearest person month worked:	4.7 (For the first year of the project)
Contribution to Project:	Configured test apparatus and performed testing
Funding Support:	

Name:	Pavan Nuthi
Project Role:	Researcher
Researcher Identifier:	
Nearest person month worked:	3.8 (For the first year of the project)
Contribution to Project:	Performed Control software and algorithms development and testing
Funding Support:	

Name:	Prashant Savant
Project Role:	Student Intern
Researcher Identifier:	
Nearest person month worked:	5.7 (For the first year of the project)
Contribution to Project:	Fabricated and tested air cells for the cushion
Funding Support:	

Name:	Nikita Deepak
Project Role:	Student Intern
Researcher Identifier:	
Nearest person month worked:	3.7 (For the first year of the project)
Contribution to Project:	Fabricated and tested air cells for the cushion
Funding Support:	

University of Pittsburgh Participants

Name:	Rory Cooper
Project Role:	U. PITT (Sub award) PI
Researcher Identifier:	
Nearest person month worked:	1.2 (For the first year of the project)
Contribution to Project:	Dr. Cooper has performed work in feedback for cushion design, literature review, and design of sensorized anthropomorphic model, PITT project management and report writing.
Funding Support:	

Name:	Hongwu Wang
Project Role:	U. PITT (Sub award) Co-I
Researcher Identifier:	
Nearest person month worked:	1.2 (For the first year of the project)
Contribution to Project:	Dr. Wang has performed work in feedback for cushion design, literature review, and design of sensorized anthropomorphic model, PITT project management, communication between PITT and UTARI, and report writing.
Funding Support:	

Name:	Garrett Grindle
Project Role:	Engineer
Researcher Identifier:	
Nearest person month worked:	1.2 (For the first year of the project)
Contribution to Project:	Mr. Grindle has performed work in the sensorized anthropomorphic model design, conceptualized and CAD models drawing.
Funding Support:	

Name:	Josh Brown
Project Role:	Electrical Engineer
Researcher Identifier:	
Nearest person month worked:	2.4 (For the first year of the project)
Contribution to Project:	Mr. Brown has performed work in the sensorized anthropomorphic model design especially the electronics and strain gauges locating and design.
Funding Support:	

Name:	Dalton Relich
Project Role:	Fabrication Technician
Researcher Identifier:	
Nearest person month worked:	2.4 (For the first year of the project)
Contribution to Project:	Mr. Relich has performed work in the area of fabrication perspective of the sensorized anthropomorphic model design and materials preparation.
Funding Support:	

- **Has there been a change in the active other support of the PD/PI(s) or senior/key personnel since the last reporting period?**

Added support commitment after receiving the CDMRP contract:

1. PI Muthu Wijesundara receive NSF grant (1605635) As a Co-PI that requires a 0.2 month/year of his time
2. PI Muthu Wijesundara received NIH grant (1R15HL129201-01A1) as Co-PI which requires 0.8 month/year of his time

Subtracted support commitment after receiving the CDMRP contract

1. PI Muthu Wijesundara's time commitment was reduced to Zero from 0.4 month/year for the NSF grant (1208623)
2. PI Muthu Wijesundara's time commitment was reduced to Zero from 1.2 month/year for the Coulter Foundation grant on Bioengineered Smart-Glove Regenerative Healing of Extremity Trauma

- **What other organizations were involved as partners?**

None

8 SPECIAL REPORTING REQUIREMENTS

Quad chart (see appendix)

9 APPENDICES

- Quad chart

Automated Seat Cushion for Pressure Ulcer Prevention Using Real-Time Mapping, Offloading, and Redistribution of Interface Pressure
SCI140265
W81XWH-15-1-0719

PI: Muthu Wijesundara **Org:** University of Texas Arlington Research Institute **Award Amount:** $741,767

Study/Product Aim(s)

- Aim 1: Design and prototype a seat cushion using sensorized bubble actuators capable of real-time pressure mapping and modulation.
- Aim 2: Conduct numerical and experimental studies on interface pressure and shear forces using an anthropomorphic model to develop a control algorithm.

Approach

Develop an automated seat cushion prototype with real-time pressure mapping coupled with selective pressure offloading and dynamic redistribution. The seat cushion consists of a sensorized pressure actuator array and an associated control unit and a GUI for planning pressure modulation. The seat cushion prototype will be evaluated using a sensorized anthropomorphic model for examining pressure mapping, offloading, and redistribution capabilities.

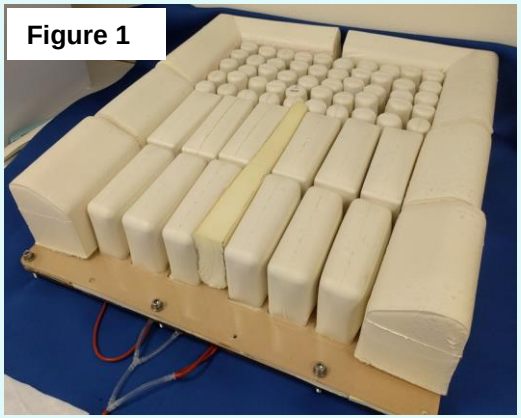

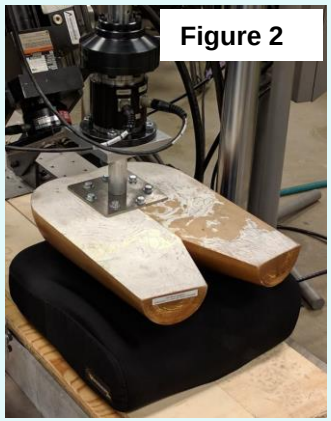

Figure 1. Full seat cushion prototype including cylindrical and rectangular bubble arrays along with foam sidewalls.
Figure 2. Seat cushion test setup with unsensorized anthropomorphic model.

Timeline and Cost

Activities / CY	15	16	17	18
Produce seat cushion prototype				
Produce anthropomorphic model				
Develop a control unit and a GUI				
Test the seat cushion prototype				
Estimated Budget ($K)	**$83**	**$318**	**$273**	**$72**

Updated: (10/28/16)

Goals/Milestones
CY15 Goal – Design seat cushion prototype
☑ Finalized the seat cushion prototype design
CY16 Goals – Realize seat cushion prototype and anthropomorphic model
☑ Realize a seat cushion prototype
☐Realize a sensorized anthropomorphic model
CY17 Goal – Build an associated control unit and evaluate the prototype
☐Develop a control unit and a GUI
☐Evaluate the seat cushion prototype experimentally and numerically
☐Develop pressure modulation plan
CY18 Goal – Perform laboratory test
☐ Test the pressure modulation capability in a laboratory environment
Comments/Challenges/Issues/Concerns
- No timeline changes to report
- Actual expenditures not up-to-date due to pending charges and a slower financial update

Budget Expenditure to Date
Projected Expenditure: $313,266
Actual Expenditure: $260,303